

Synchronisation schemes for two dimensional discrete systems

G. Ambika and K. Ambika

Department of Physics, Maharaja's College, Cochin-682011, India.

E-mail: ambika@iucaa.ernet.in, ambikak2002@yahoo.com

Abstract. In this work we consider two models of two dimensional discrete systems subjected to three different types of coupling and analyse systematically the performance of each in realising synchronised states. We find that linear coupling effectively introduce control of chaos along with synchronisation, while synchronised chaotic states are possible with an additive parametric coupling scheme both being equally relevent for specific applications. The basin leading to synchronisation in the initial value plane and the choice of parameter values for synchronisation in the parameter plane are isolated in each case.

PACS numbers: 05.45.Gg; 0.5.45.Xt

Keywords: synchronisation, stability, Gumowski-Mira map, additive and parametric coupling

1. Introduction

The presence of chaos has been extensively demonstrated in many naturally occurring nonlinear systems. The capability of the chaotic state to amplify small perturbations improves their utility for reaching specific desired states with very high flexibility and low energy cost. However there are many situations like power systems where control of chaos is desirable. This helps in improving a desired behaviour by making only small time dependant perturbations in a system parameter. In this context, a key observation is that a chaotic attractor has embedded within it an infinite set of unstable periodic orbits and the control mechanism aims at stabilising the system to any chosen one among them. The theoretical and experimental works so far done on this topic shows that various methods of control are capable of leading to improved performance and ordered response [1]. Moreover the naturally occurring chaotic orbits on a dynamical attractor has been utilised to carry information [2]. Thus one can encode and transmit a prescribed message using chaotic states. This process may offer practical advantages over the usual periodic carriers, such as the possibility of real time reconstructions of signal dropouts in the communication. In such cases, it is desirable to have a number of systems behaving in a synchronised manner and this is achieved by coupling or feedback between systems.

The phenomenon of synchronisation in chaotic systems has received much attention since 1990 [3]. It is found to occur in the dynamics of many coupled physical [4, 5, 6, 7, 8, 9] and biological systems [10, 11, 12] such as neurons in a network [13, 14, 15, 16]. The synchronisation schemes form the basis of biological clocks that regulate daily and seasonal rhythms of living systems from bacteria to humans. Even when the individual systems are in the realm of chaotic behaviour, the coupled one most often can be synchronised in periodic or regular states. Thus synchronisation techniques automatically brings in control of chaos also. However there are applications like information processing where synchronised chaotic states are desirable.

There are different types of synchronised states [17, 18] occuring in coupled chaotic systems. The first type called complete synchronisation has received much attention with the development of a new type of communication technique that exploits the possibility of masking a message by mixing it with a chaotic signal [19]. With both the amplitudes and phases of the coupled systems varying in the same way the synchronised chaotic state will be restricted to a smooth invariant manifold of lower dimension than the full phase space. Complete synchronisation implies that the details of the two systems are identical or their difference converges to zero. [1, 20, 21, 22]. However there are situations where one observes lag synchronisation in which the system states coincide only when one of them is shifted in time. So also there are cases of generalised partial synchronisation where no amplitude synchronisation is observed but the average amplitude is bounded and varies periodically [23].

The majority of the research works reported in the literature have been focused on synchronisation of continuous systems and a few on discrete systems concentrate on

one dimensional map [19, 20, 21]. In this paper we consider two dimensional discrete systems and introduce different coupling schemes and the resulting possible types of synchronisation. Such systems model many interesting situations like population dynamics of mutually dependent species, neural networks, image processing techniques etc. Hence the possibility of their evolution in a synchronised manner under different types of connectivity forms a useful study. Moreover, two dimensional discrete systems occur as the Poincaré maps of three dimensional continuous systems, which are the lowest dimensional systems capable of exhibiting chaos. Hence the synchronised behaviour of the latter can be analysed in a general and systematic way using the former.

The paper is organized as follows. In § 2, we describe the different coupling schemes and discuss the stability of synchronisation for each one. In § 3 and § 4 these coupling schemes are applied to two specific examples of discrete systems *viz.* Gumowski-Mira map (GM) and Modified Gumowski-Mira map (MGM) maps and their synchronisation is studied using similarity function, stability analysis, synchronisation and stabilisation times and available basin in the parameter as well as initial value plane. It is found that complete synchronisation with control, lag synchronisation and synchronised chaotic states can be realised by choosing different coupling techniques. Concluding remarks are given in § 5.

2. Coupling schemes for 2-d maps

We start with a two dimensional discrete system which is written as

$$\overline{X1} = \overline{F}(\overline{X1}, \mu) \text{ and } \overline{X2} = \overline{F}(\overline{X2}, \mu). \quad (1)$$

where $\overline{X1} = (X1, Y1)$ define two dimensional space of the first map, $\overline{X2} = (X2, Y2)$ the two dimensional space of the second map and μ is the control parameter. When both the systems are coupled the dynamics of the system develops as

$$\begin{aligned} \overline{X1} &= \overline{F}(\overline{X1}, \mu) + I_1(\epsilon, \overline{X1}, \overline{X2}) \\ \overline{X2} &= \overline{F}(\overline{X2}, \mu) + I_2(\epsilon, \overline{X1}, \overline{X2}) \end{aligned} \quad (2)$$

Here I_1 or I_2 is the coupling scheme applied to both the maps which in general is a function of the variables of both maps and the coupling parameter ϵ . Different types of I can be chosen to achieve the required synchronised state.

The possible forms for the coupling scheme I that we consider in this work are

(i) linear coupling (CS1) applied to one of the equations, *ie.*

$$I_i = \epsilon X_j$$

(ii) linear difference coupling (CS2), $I_i = \epsilon(X_j - X_i)$

(iii) additive parametric coupling (CS3), $I_i = \mu(1 - \epsilon X_j)$.

For all the above cases $i, j = 1, 2$ and $i \neq j$.

The first two are well studied schemes of synchronisation while the third one is introduced for the particular type of two dimensional system discussed here. It is

interesting to note that this coupling depends on the parameter μ of the individual system in addition to the usual coupling parameter ϵ . We find that this introduces more flexibility in the scheme by providing two parameters, one of which controls the dynamics also. This can result in a wider range in the (μ, ϵ) plane for optimum synchronisation. The stability analysis is carried out and the similarity function plotted against time to characterise the nature and robustness of the synchronised state. In each case the efficiency of the scheme is quantified by computing the average time τ_1 taken for achieving synchronisation over a number of initial conditions. The robustness is checked by perturbing the synchronised state with a random noise and computing the stabilisation time τ_2 required to regain synchronisation after perturbation.

Regions in the parameter plane (μ, ϵ) that leads to different synchronised states are isolated and the basin of synchronisation in the phase plane marked out. These characterisations help to estimate the relative merits of different schemes.

The stability of the symmetric state $X_i = X_j$ and $Y_i = Y_j$ with respect to the transverse perturbations $(\delta\bar{X}, \delta\bar{Y})$ is analysed by linearisation. We get

$$\begin{aligned}\delta\bar{X}1 &= \frac{\partial F}{\partial X1}\delta X1 + \frac{\partial F}{\partial Y1}\delta Y1 + \epsilon\bar{C}(\delta\bar{X}2, \delta\bar{X}1) \\ \delta\bar{X}2 &= \frac{\partial F}{\partial X2}\delta X2 + \frac{\partial F}{\partial Y2}\delta Y2 + \epsilon\bar{C}(\delta\bar{X}1, \delta\bar{X}2)\end{aligned}\quad (3)$$

where \bar{C} is in general a function of $\delta\bar{X}1, \delta\bar{X}2$. Defining $\bar{V} = (\delta\bar{X}1 - \delta\bar{X}2)$ and $F_{ij} = \frac{\partial F_i}{\partial X_j}$.

(i) For linear coupling this is obtained as

$$V_{n+1}^i = \sum_j F_{ij} V_n^j - \epsilon C_i \text{ with } C_1 = 1, C_2 = 0, i = 1, 2. \quad (4)$$

(ii) For linear difference coupling,

$$V_{n+1}^i = \sum_j F_{ij} V_n^j - 2\epsilon C_i \quad (5)$$

with $C_1 = 1$ and $C_2 = 0$.

(iii) For additive parametric coupling,

$$V_{n+1}^i = \sum_j F_{ij} V_n^j + \mu\epsilon C_i \text{ with } C_1 = 1, C_2 = 1. \quad (6)$$

Eigen values σ^i of the Jacobian matrix F_{ij} are evaluated and the transverse Lyapunov exponents (λ_\perp) calculated.

For CS1,

$$\lambda_\perp^i = \ln(\sigma^i - \epsilon). \quad (7)$$

For CS2,

$$\lambda_\perp^i = \ln(\sigma^i - 2\epsilon). \quad (8)$$

For CS3,

$$\lambda_\perp^i = \ln(\sigma^i + \mu\epsilon). \quad (9)$$

The largest transverse Lyapunov exponent being less than zero indicates the stability of the synchronised state [19].

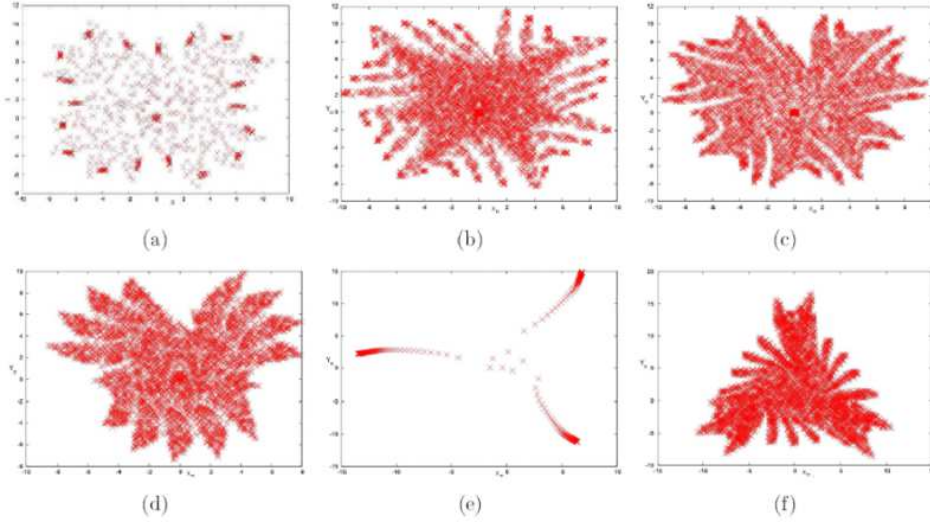


Figure 1. GM patterns generated in the phase space ie. (X, Y) plane by the discrete system in equation (10). Here $a = 0.008$, $b = 0.05$, $X = 0.1$, $Y = 0.0$. $-0.6 \leq \mu \leq -0.1$, $\Delta\mu = 0.1$. It is clear that the asymptotic dynamic states depends very sensitively on the control parameter μ .

3. Synchronisation in Gumowski-Mira maps

As a first example of a two dimensional discrete map we consider Gumowski-Mira Map (GM)[24]. This is a two dimensional difference equation in (X, Y) involving a non linear function $f(X)$ that is advanced in time by one iteration in the Y equation. The iterates of this map give rise to a variety of interesting patterns in the (X, Y) plane and hence useful as a two dimensional iterative scheme for producing fractal objects. The GM transformation is defined in the (X, Y) plane as

$$\begin{aligned} X_{n+1} &= Y_n + a(1 - bY_n^2)Y_n + f(X_n) \\ Y_{n+1} &= -X_n + f(X_{n+1}) \\ \text{with } f(X_n) &= \mu X_n + \frac{2(1 - \mu)X_n^2}{1 + X_n^2}. \end{aligned} \tag{10}$$

This map is found to have a very sensitive dependence on the control parameter μ [25, 26]. The phase space plots known as GM patterns in Fig. (1a) justify this. In these calculations a and b are fixed to be 0.008 and 0.05 respectively and μ is increased in steps of 0.1. In an earlier analysis we have found that many recurring periodic and self similar sub structures, each with its own intermittency, periodicity, quasi periodic bands, band merging etc. in the bifurcation scenario of the system [26] explain the dynamics of these patterns.

Here we apply different coupling schemes mentioned in the previous section to the above system and try to target it to lower stable periodicities in their synchronised states.

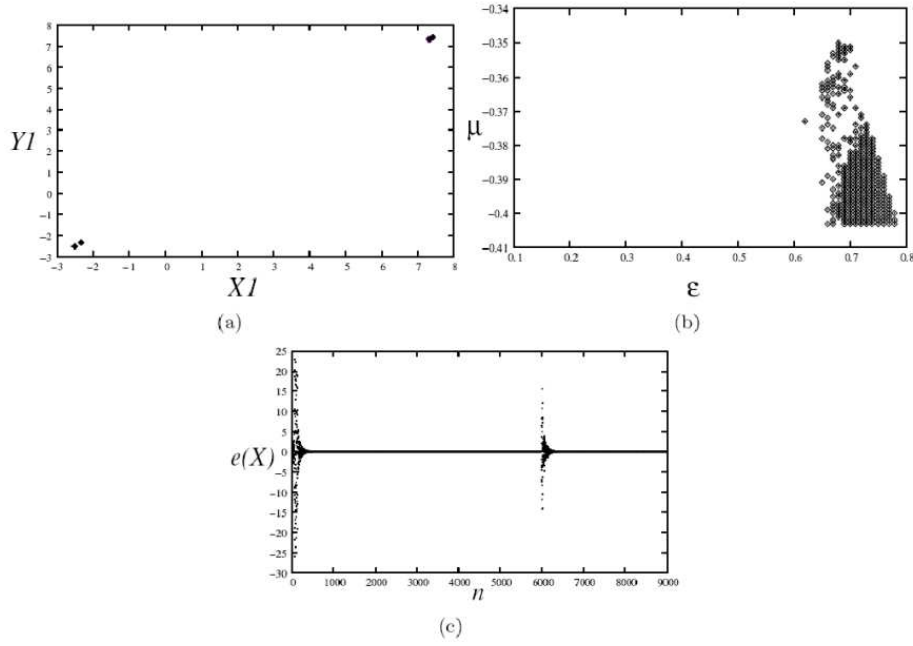


Figure 2. Linear coupling applied to two GM maps a) The synchronised four cycle for $\mu = -0.39$. b) The points in the (μ, ϵ) plane that lead to synchronised four cycle. c) The error function $e(X)$ plotted against iteration time n . When a random perturbation is applied after 6000 iterations synchronisation is regained in 410 steps.

In the case of CS1 the pair of synchronising systems evolve as

$$\begin{aligned}
 X1_{n+1} &= Y1_n + a(1 - bY1_n^2)Y1_n + f(X1_n) + \epsilon X2_n \\
 Y1_{n+1} &= -X1_n + f(X1_{n+1}) \\
 X2_{n+1} &= Y2_n + a(1 - bY2_n^2)Y2_n + f(X2_n) + \epsilon X1_n \\
 Y2_{n+1} &= -X2_n + f(X2_{n+1})
 \end{aligned} \tag{11}$$

where ϵ is the coupling parameter. The advantage of the method is that the feedback in the X equation alone suffices to achieve total synchronisation of both the variables. We start with $\mu = -0.39$ (the individual systems are in the chaotic region), for $\epsilon = 0.7$ and initial conditions $(0.1, 0.0)$, $(0.2, 0.12)$, the X and Y equations of both settle to an identical four cycle which is clear from Fig.(2a). Fig (2b) gives the (μ, ϵ) plot for synchronising values. The error function defined as $e(X) = X1 - X2$ and $e(Y) = Y1 - Y2$ tends to zero when synchronisation is achieved [27]. We test this numerically by iterating equation (11) for values mentioned above and plotting $e(X)$ against iteration number n (Fig (2c)). The synchronisation time τ_1 and stabilisation time τ_2 which is the time taken to stabilise after applying a random noise for 10 iterations are shown in the figure. The values of τ_1 and τ_2 are found for 10 different initial conditions and their average calculated. We get $\tau_1 = 778$ and $\tau_2 = 410$. The largest transverse Lyapunov exponent for the four cycle works out to be -0.1564 . This indicates that this synchronised state is stable.

However this coupling is active even after achieving synchronisation. Hence to make

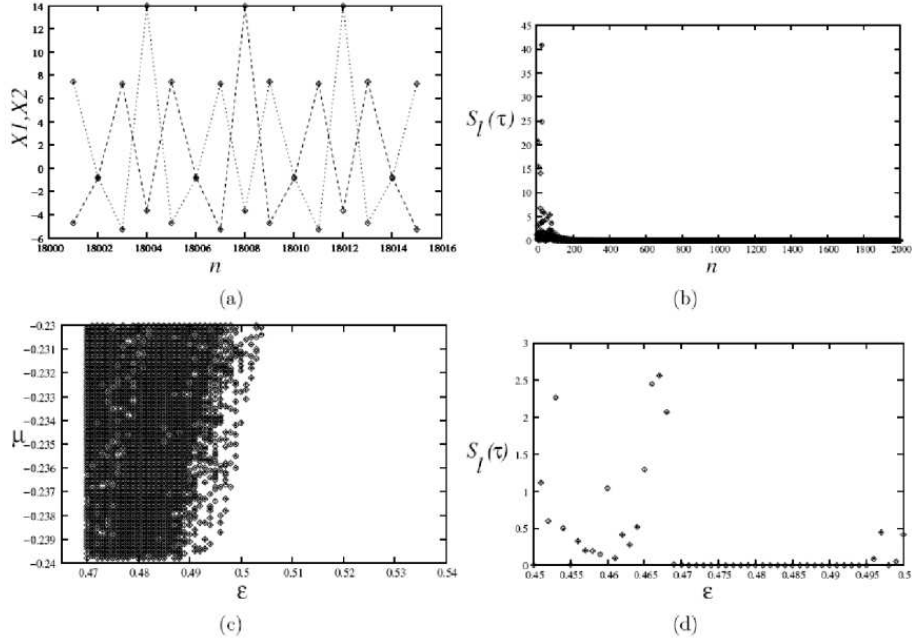


Figure 3. Lag synchronisation observed in GM maps under Linear difference coupling
a) $(X1, X2)$ plot with iteration number n showing synchronisation with a lag of $\tau = 4$.
b) Variation of similarity function with iteration number n for $\tau = 4$. c) Regions in the (μ, ϵ) plane that can lead to lag synchronisation. d) Variation of similarity function as a function of coupling parameter ϵ plotted after 10000 steps for $\mu = -0.23$. Lag synchronisation is realised only for a range of $0.471 < \epsilon < 0.495$.

the scheme cost effective, we try a linear difference coupling (CS2) of the two systems,

$$\begin{aligned}
X1_{n+1} &= Y1_n + a(1 - bY1_n^2)Y1_n + f(X1_n) + \epsilon(X2_n - X1_n) \\
Y1_{n+1} &= -X1_n + f(X1_{n+1}) \\
X2_{n+1} &= Y2_n + a(1 - bY2_n^2)Y2_n + f(X2_n) + \epsilon(X1_n - X2_n) \\
Y2_{n+1} &= -X2_n + f(X2_{n+1})
\end{aligned} \tag{12}$$

With $\mu = -0.23$ both the systems are individually chaotic. When $\epsilon = 0.48$ and initial conditions $(0.1, 0.0), (0.2, 0.12)$ they stabilise to an eight cycle, with a time lag $\tau = 4$ between them. Synchronisation achieved here is lag synchronisation which can be confirmed using similarity function, defined as [28]

$$S_l(\tau) = \frac{\langle [X2_{n+\tau} - X1_n]^2 \rangle}{[\langle X1_n^2 \rangle \langle X2_n^2 \rangle]^{1/2}} \tag{13}$$

For a non zero value of τ , $S_l(\tau) \rightarrow 0$ corresponds to lag synchronisation. It is clear from Fig (3a), the time series plot of $(X1_n, X2_n)$ with $\tau = 4$. Fig (3b) gives the $S_l(\tau)$ vs n plot which establishes lag synchronisation phenomena in the system. Fig (3c) gives the (μ, ϵ) plot for synchronising values. Fig (3d) gives the variation of similarity function $S_l(\tau)$ with ϵ . It is seen that lag synchronisation occurs only in a narrow region of ϵ and the states are de-synchronised in the remaining regions. The largest transverse Lyapunov exponent, $\lambda_{\perp} = -0.431144$, for the state with lag synchronisation.

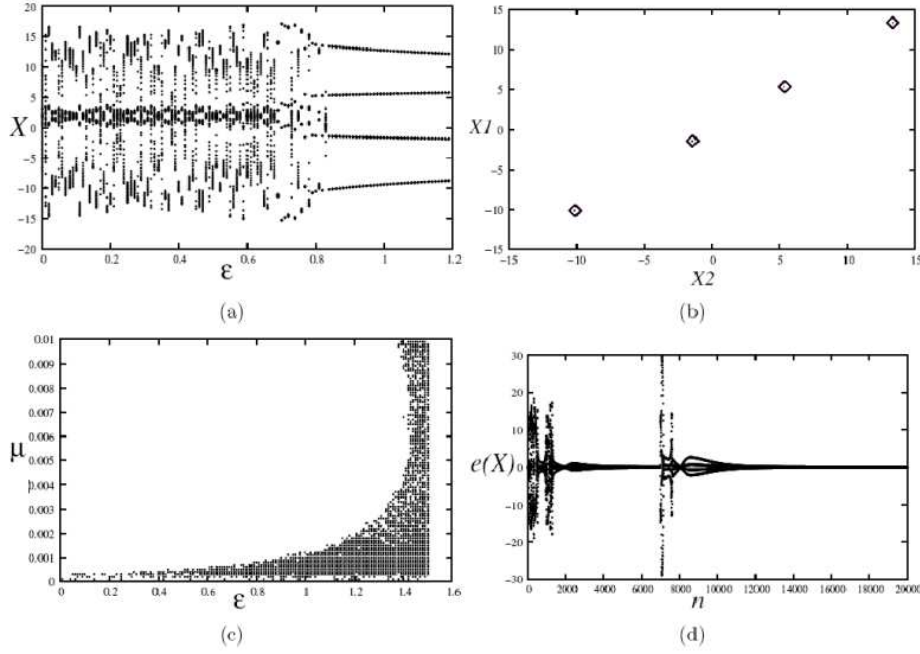


Figure 4. Additive parametric coupling applied in two GM maps for $\mu = 0.001$ a) ϵ vs $X1$ plot; the two system settles to four cycle for $\epsilon = 0.8$ indicating control of chaos before the onset of synchronisation; b) The synchronised periodic four cycle as ϵ is increased to 0.85; c) The values in the (μ, ϵ) plane that leads to synchronisation in the periodic four cycle; d) The evolution of the error function $e(X)$ showing complete synchronisation and return to synchronisation after applying the random perturbation at the 7000th step.

The synchronisation in this scheme is only lag type. To achieve total synchronisation in a periodic state we try an additive parametric coupling (CS3).

The dynamics of the coupled GM maps on applying CS3 develops through the equations

$$\begin{aligned}
 X1_{n+1} &= Y1_n + a(1 - bY1_n^2)Y1_n + f(X1_n) + \mu(1 - \epsilon X2_n) \\
 Y1_{n+1} &= -X1_n + f(X1_{n+1}) + \mu(1 - \epsilon Y2_n) \\
 X2_{n+1} &= Y2_n + a(1 - bY2_n^2)Y2_n + f(X2_n) + \mu(1 - \epsilon X1_n) \\
 Y2_{n+1} &= -X2_n + f(X2_{n+1}) + \mu(1 - \epsilon Y1_n).
 \end{aligned} \tag{14}$$

For $\mu = 0.001$, both the maps individually exhibit irregular and aperiodic behaviour. After coupling with $\epsilon = 0.85$ and initial values $(0.1, 0.0)$, $(0.2, 0.12)$ they are found to settle to the same four cycle. Fig (4a) gives the (ϵ, x) plot for the first map which shows that for $\epsilon = 0.8$ the map settles to a four cycle *ie.* control of chaos is taking place before synchronisation and synchronisation is reached only when ϵ is increased to 0.85. Fig (4b) gives the $(X1, X2)$ plot showing synchronisation and in fig (4c) the values of μ and ϵ for which synchronisation is achieved are shown.

The variation of the error function is calculated numerically by iterating equation (14) and is plotted against iteration number n in Fig (4d). The average time taken for

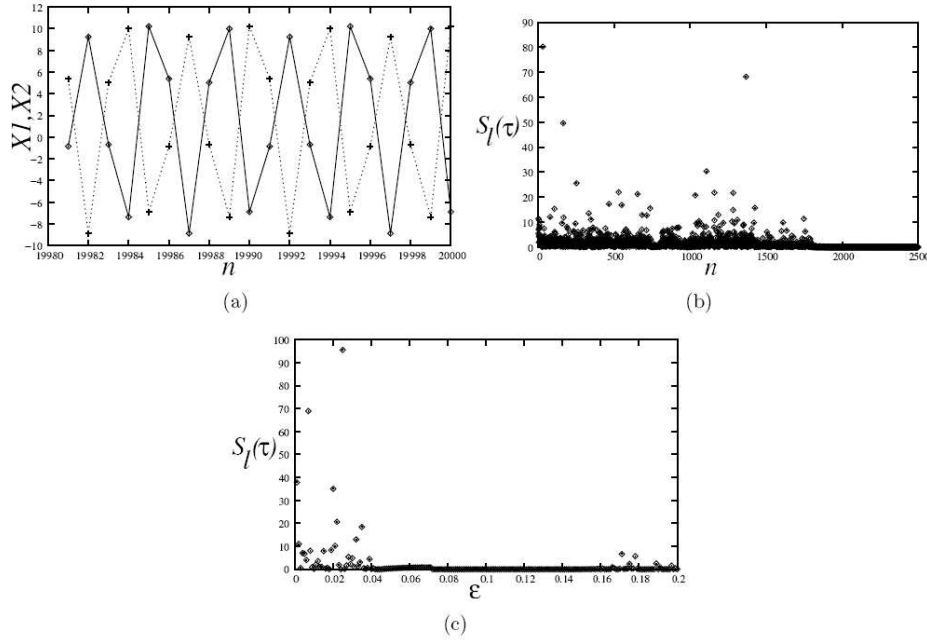


Figure 5. The lag synchronisation observed under additive parametric coupling for $\epsilon = 0.1$, $\mu = -0.3$ with an asymptotic 10 cycle (a) X_1 and X_2 plotted with iteration number n showing a lag of $\tau = 5$; (b) the variation of the similarity function to zero after $n = 1800$ (c) the variation of similarity function as a function of coupling parameter ϵ . Lag synchronisation is realised in the range $0.075 < \epsilon < 0.15$.

synchronisation is found to be $\tau_1 = 6265$ and the average stabilisation time $\tau_2 = 3844$. The largest transverse Lyapunov exponent is calculated as explained in the previous case and is obtained as $\lambda_{\perp} = -2.75098$. Thus the synchronised state is a periodic four cycle which is stable.

With $\mu = -0.3$, initial conditions $(0.1, 0)$, $(0.2, 0.12)$ and $\epsilon = 0.1$ both the systems are found to synchronise to a stable ten cycle. We note that this is also a case of lag synchronisation *ie.*, $X_{1n} = X_{2n+\tau}$, with $\tau = 5$. The time series plot of X_{1n} and X_{2n} in Fig (5a) and $S_l(\tau)$ vs n plot in Fig (5b) establishes this phenomenon in the system. We observe lag synchronisation for the range $0.075 < \epsilon < 0.15$ (Fig (5c)).

The range over which lag synchronisation exists in this case is larger than the previous type of coupling. However beyond $\epsilon = 0.15$, the two systems are totally desynchronised.

4. Synchronisation in Modified Gumowski-Mira maps

As a second example we consider a variant of the GM map which is hereafter called modified GM map (MGM map), defined by the following set of equations.

$$\begin{aligned} X_{n+1} &= Y_n + a(1 - bY_n^2)Y_n + f(X_n) \\ Y_{n+1} &= -X_n + f(X_n) \end{aligned} \quad (15)$$

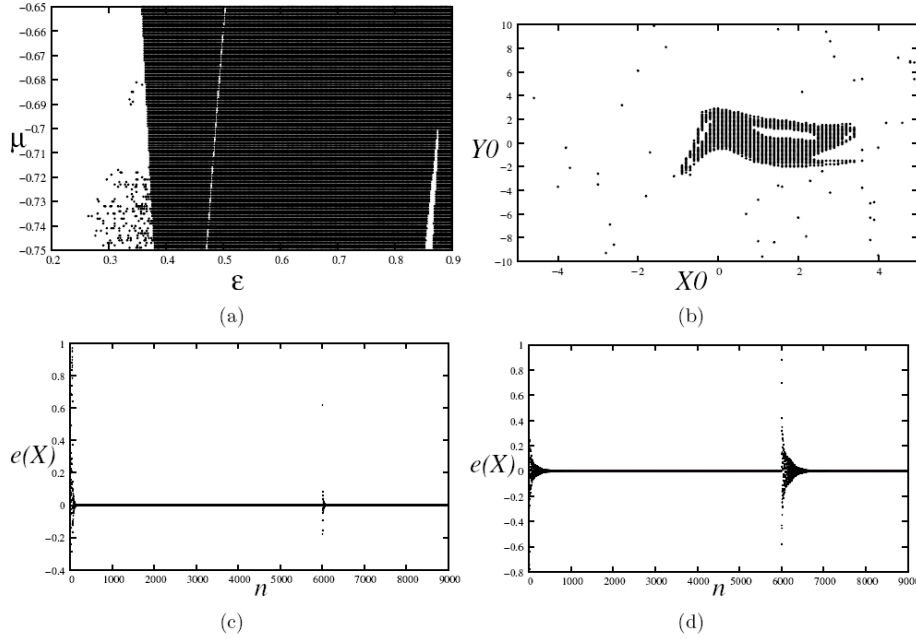


Figure 6. Linear coupling applied to two MGM maps a) Regions in (μ, ϵ) plane leading to synchronised states. b) basin of the synchronised states in the initial value plane. c) error function $e(X)$ vs iteration number n plot for $\epsilon = 0.4$ where the synchronised state is a fixed point. A random noise is applied at the 6000th iterate. Synchronisation is regained after 98 iterations. d) error function $e(X)$ vs n plot for $\epsilon = 0.5$ where the synchronised state is a limit cycle. A random noise is applied at the 6000th iterate. Synchronisation is regained after 520 iterations.

$$\text{with } f(X_n) = \mu X_n + \frac{2(1 - \mu)X_n^2}{1 + X_n^2}.$$

In this map the iterations in both X and Y are in step. With values of a and b are fixed as $a = 0.008$, $b = 0.05$, the system has a prominent period doubling sequence in the bifurcation scenario [29]. In the GM map considered in § 3 above synchronised states are periodic states which means synchronisation follows control of chaos. We find that synchronised chaotic states can be realised in addition to synchronised fixed points and limit cycles in the modified GM map introduced here.

We apply CS1 to two such systems. In this case for $\mu = -0.7$ and initial conditions $(0.1, 0)$, $(0.2, 0.1)$ both the maps are individually chaotic. With coupling for $\epsilon = 0.4$ they asymptotically approach a fixed point $(1.66, -0.3316)$, while for $\epsilon = 0.5$ they synchronise to a limit cycle.

Fig (6a) gives the (μ, ϵ) plot where synchronisation sets in. The region to the left of the white line corresponds to synchronisation to a fixed point while that to the right corresponds to limit cycle. Fig (6b) gives the basin of synchronisation of two MGM maps for $\epsilon = 0.5$ (when the final synchronised state is a limit cycle). Fig (6c) and Fig (6d) gives the $e(X) - n$ plot of coupled MGM maps from where synchronisation time and stabilisation time can be read off. For $\mu = -0.7$ and $\epsilon = 0.4$ the largest transverse Lyapunov exponent (λ_{\perp}) is (-1.883383) where one cycle periodicity is seen

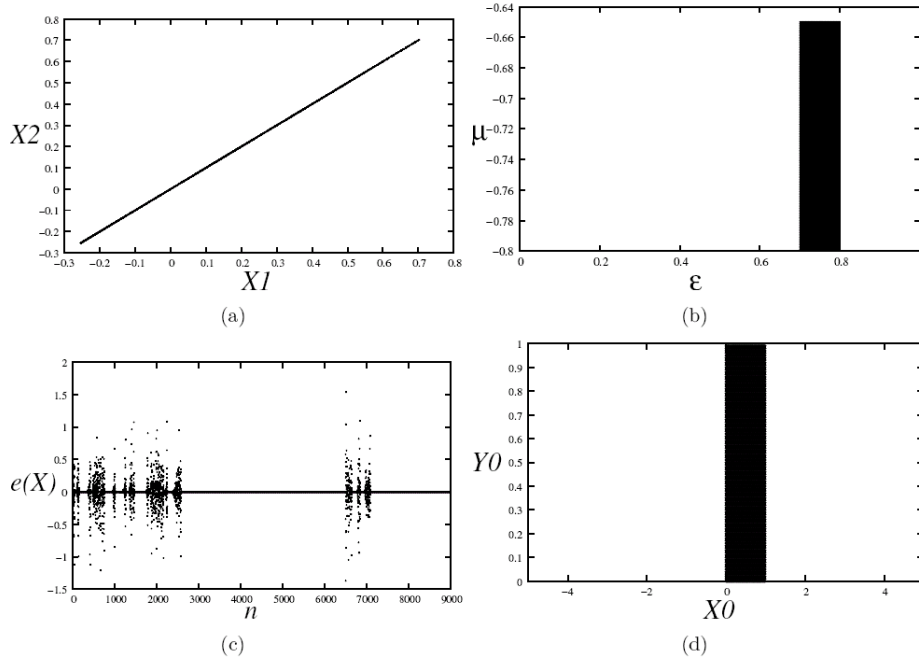


Figure 7. Linear difference coupling applied to two MGM maps. a) $(X1, X2)$ plot showing synchronised chaotic states b) regions in the (μ, ϵ) plane where synchronisation occurs. c) Variation of the error function $e(X)$ with n for $\mu = -0.7$. The time taken to reach synchronisation and the time taken to regain the same after a noisy perturbation are more in this case d) basin of synchronised chaotic state in the initial value plane.

in the synchronised state. For $\epsilon = 0.5$ when the synchronised state is a limit cycle the value λ_{\perp} is (-1.44478) .

We try CS2 for two MGM maps. For $\mu = -0.7$ both the systems are individually chaotic and for $\epsilon = 0.85$ we observe chaotic states synchronised in the coupled system. This is shown in $(X1, X2)$ plot in Fig (7a). Fig (7b) gives the regions in the (μ, ϵ) plane leading to this type of synchronisation. Error function $e(X)$ and $e(Y)$ evolve into a stable fixed point $(0, 0)$, which is shown in Fig (7c). The average synchronisation time and stabilisation time for 10 different initial conditions are found to be $\tau_1 = 2605$ and $\tau_2 = 1057$. Fig (7d) gives the basin for synchronisation in the range $[-5, 5]$. $\lambda_{\perp} = -0.40786$ shows that the chaotic synchronised state is stable.

We try CS3 scheme to two MGM maps.

Here for $\mu = -0.3$ initial conditions $(0.1, 0.0)(0.2, 0.1)$ (where individual systems show 4 cycle periodicity) for $\epsilon = 0.5$, we observe synchronised chaotic states in the coupled systems. This is shown in $(X1, X2)$ plot in Fig (8a). Fig (8b) gives the regions of the parameter plane (μ, ϵ) leading to this type of synchronisation.

$e(X)$ evolve into a stable fixed point $(0, 0)$ which is shown in Fig (8c). A similar plot is obtained for $e(Y)$ also. Time taken for synchronisation $\tau_1 = 282$. After 2000 iterations a noise is applied and stabilisation time is obtained as $\tau_2 = 186$. Fig (8d) gives the basin for synchronisation in the range $[-5, 5]$.

For this coupling, the largest transverse Lyapunov exponent computed works out

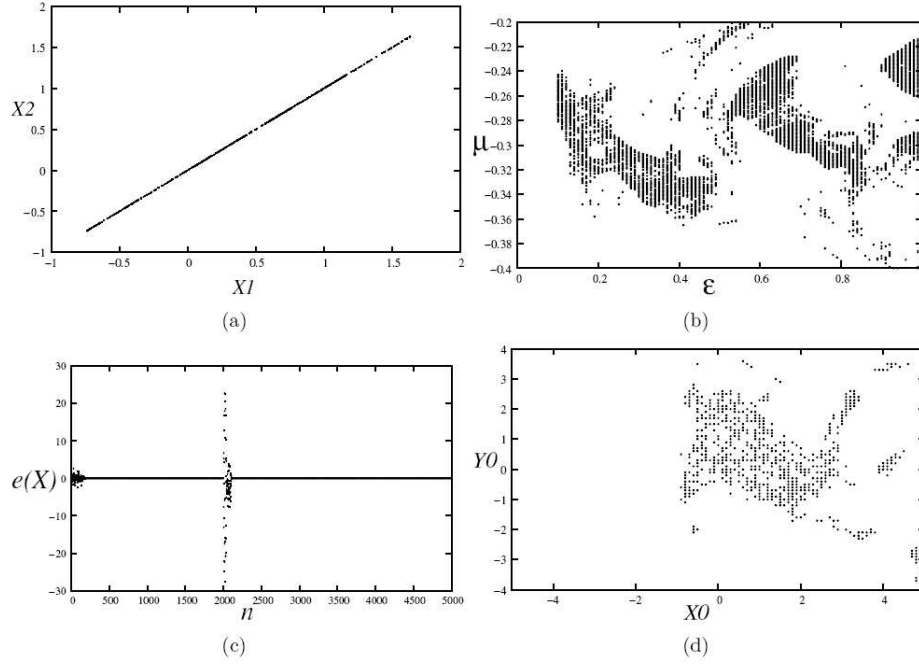


Figure 8. Additive parametric coupling in two MGM maps a) The (X_1, X_2) plot of the synchronised chaotic state b) points in the (μ, ϵ) plane resulting in synchronisation. c) Variation of error function $e(X)$ with time for $\mu = -0.3$. d) The basin of synchronised chaotic state in the initial value plane. This scheme is more efficient and the state is robust to perturbation.

to be -1.227154 indicating stability for synchronised chaotic state.

5. Conclusion

In this work, a study on different coupling schemes for synchronisation in two dimensional systems is carried out. We consider two types of two dimensional discrete maps called Gumowski-Mira(GM) maps and modified Gumowski-Mira(MGM) maps. Three different coupling schemes namely linear coupling(CS1), linear difference coupling(CS2) and additive parametric coupling(CS3) are applied to them. In GM maps using CS1 and CS3 control of chaos is achieved along with complete synchronisation. However only lag synchronisation is observed with CS2. In MGM maps while CS1 stabilises the maps to fixed points or limit cycles, CS2 and CS3 lead to synchronised chaotic states. It is found that the synchronisation time and stabilisation time is shortest for CS1 in GM maps compared to CS3. In the case of MGM maps also CS1 offers the shortest synchronisation time and stabilisation time. In this case both CS2 and CS3 yields chaotic synchronised states among which τ_1 and τ_2 are shorter for CS3. It is found that the basin of synchronisation in the initial value plane is unique for all the three types of coupling in GM maps, while the regions leading to synchronisation in MGM maps are small but finite. The parameter values (μ, ϵ) leading to synchronisation in GM maps has largest range for CS3 while those leading to lag synchronisation in CS2 has

limited range. In MGM maps this range is maximum for CS1 and minimum for CS2. It is found that although CS2 is cost effective, CS1 gives maximum range in (μ, ϵ) plane, wider basin in $(X0, Y0)$ plane and shorter times for synchronisation and stabilisation after perturbation. CS3 has wider range in parameter with control of chaos in GM map and is useful to get synchronised chaotic states in MGM maps.

Although control of chaos is simultaneous with synchronisation in most cases, synchronised chaotic states are possible in the second example considered here. This may find applications in information processing using connected systems.

Acknowledgement

K. A. thanks University Grants Commission, New Delhi for deputation under Faculty Improvement Programme.

References

- [1] S. Boccaletti, C. Grelogi, Y. C. Lai, H. Maucini, D. Maza “The control of chaos: Theory and Applications”, *Phy. Rep.* **329**, 103, (2000).
- [2] J. Kurths, Grelogi, Y. C. Lai, Introduction: Control and Synchronisation in chaotic dynamical systems. *Chaos*, Vol. **13** Number 1 (2003).
- [3] L. Pecora, T. Carroll *Phys. Rev. Lett.* **64**, (1990), 821.
- [4] Trubetskov. D. I, Hramov. A. E. *Journal of Communications Technology and Electronics* **48**, 105, (2003).
- [5] Tang. D.Y., Dykstra R, Hamilton M. W, Heckenberg. N.R., *Phys. Rev.* **E. 57**, 3649 (1998).
- [6] Rosa. E., Pardo. W. B., Ticos. C. M., Wakenstein. J. A., Monti. M., *Int. J. Bifurcation and Chaos* **10**, 2551 (2000).
- [7] Ticos. C. M., Rosa. E., Pardo. W. B., Walkenstein. J. A., Monti. M., *Phys. Rev. Lett.* **85**, 2929 (2000).
- [8] Arecchi F. T., Allaria. E, Garbo. A. D, Menucci. R., *Phys. Rev. Lett.* **86**, 791 (2001).
- [9] Junge. L, Parlitz. V., Lauterlorn. W, *Phys. Rev.* **E 54**, 2115 (1996).
- [10] Tass. P. A. et. al. *Phys. Rev. Lett.* **81**, 3291, (1998).
- [11] Anishchenko V. S, Balanov, A. G, Janson. N. B, Igosheva. N. B., Bordyugov. G. V., *Int. J. Bifurcation and Chaos* **10**, 2339, (2000).
- [12] Prokhorov et. al. *Phys. Rev.* **E. 68**, 041913, (2003).
- [13] N.F. Rulkov, *Chaos* **6**, 262, (1996).
- [14] Elson. R. C., et. al, *Phys. Rev. Lett.* **81**, 5692, (1998).
- [15] Tass. P. A. et. al, *Phys. Rev. Lett.* **90**, 088101, (2003).
- [16] Rulkov. N. F., *Phys. Rev.* **E 65**, 041922, (2002).
- [17] Pikovsky. A., Rosemblum. M., Kurths. J., *Int. J. Bifurcation and chaos.* **10**, 2291 (2000).
- [18] Pecora. L. M., Carroll. T. L., *Phys. Rev. A*, **44**, 2374 (1991).
- [19] Pikovsky A., Rosenblem M., Kurths. J., *Synchronisation: a universal concept in nonlinear sciences* (Cambridge University Press, 2001).
- [20] Murali. K., Lakshmanan. M., *Phys. Rev.* **E 49**, 4882 (1994).
- [21] Murali. K., Lakshmanan M., *Phys. Rev.* **E 48**, R1624 (1994).
- [22] Pecora L. M., Carroll. T. L., Johnson G. A., Mar D. J., Heagy J. F., *Chaos* **7**: 520–543, 1997c
- [23] Olga. B. , Isaeva, Sergey. P. Kuznetsov, arXiv.nlin.CD/0509012V1 6Sep2005
- [24] I. Gumowski- C. Mira (1980) *Recurrences and Discrete Dynamics Systems*, Springer Verlag.
- [25] K. Otsubo, M. Washida., T. Itoh, K. Katuara, M. Hayashi, Computer simulations on the Gumowski-Mira Transformation, *Forma* 15.

- [26] G. Ambika, K. Ambika, Intermittency and Synchronisation in Gumowski-Mira maps. communicated to Chaos, Solitons and Fractals.
- [27] Vinod Patidar, K. K. Sud, Synchronising identical chaotic systems using external chaotic driving – Proc. National Conference on Nonlinear Systems and Devices 2005, NCNSD 2005.
- [28] Rosenblem. M. G., Pikovsky. A. S., Kurths. J., *Phys. Rev. Lett.* **78**, 4193 (1997).
- [29] G. Ambika, K. Ambika, Synchronisation schemes for Gumowski-Mira maps, Nonlinear Systems and Dynamics, eds. M. Lakshmanan, R. Sahadevan, Allied Publishers Pvt. Ltd. 2006.